

FLUVIALLY-INDUCED TERRESTRIAL IMPACT CRATER DENUDATION: A DRAINAGE PERSPECTIVE

S. James¹, Saranya R. Chandran¹ and K.S. Sajinkumar^{1,2}, ¹Department of Geology, University of Kerala, Thiruvananthapuram, Kerala, India (shaniajames@keralauniversity.ac.in), ²Department of Geological and Mining Engineering and Sciences, Michigan Technological University, Houghton, MI, USA.

Introduction: Terrestrial impact crater morphology is modified by both, denudational processes and plate tectonics; the latter being the main destructive agent of most craters from the Earth's surface. Terrestrial craters depict characteristic radial, centripetal and concentric drainage patterns (Fig.1.), by virtue of its morphology, and are often developed during or immediately after its formation. Fluvial agents significantly influence a crater's drainage pattern and post-impact morphology in conjunction with cumulative effects of paleoclimate, lithology and time. The study introduces a Denudation Index (DI) for terrestrial impact craters, which quantifies the extent of rim degradation resulting from fluvial action.

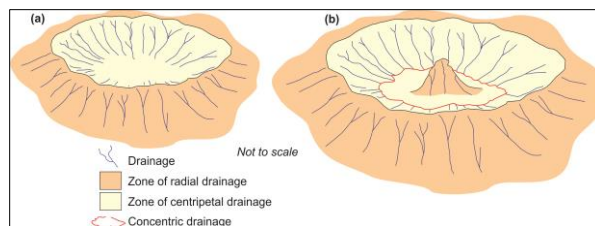


Fig.1. Drainage patterns of (a) simple (one set of centripetal and radial), (b) complex craters (two radial set; one centripetal set)

Materials and Methods: The following methodologies were carried out in the study.

1. Derivation of DI.

$$RI = \frac{(A_{out} + T_{in})}{2} \quad (1)$$

$$DI = 1 - RI \quad (2)$$

where, RI is Retention Index, A_{out} is number of 1st order streams flowing outward (i.e., radial) from rim, T_{out} is total number of 1st order streams flowing radially from rim, A_{in} is number of 1st order streams flowing inward (i.e., centripetally) from rim, and T_{in} is total number of 1st order streams flowing centripetally from rim. Fig.2. depicts DI calculation for Xiuyan crater in China.

2. Methods. Impact crater data was primarily taken from Earth Impact Database and other sources [1][2]. Craters were shortlisted for the study based on the following: (a) DEM availability (ALOS-PALSAR, TanDEM-X), (b) dominant surface expression, (c) non-submerged or unfilled. The 1st order drainage for each crater was

derived and A_{out} , T_{out} , A_{in} and T_{in} was visually interpreted and manually counted. RI and DI were calculated. Following this, the DI was correlated to target lithology data [1][3]. Paleoclimatic data was generated by reconstructing crater paleo-positions at 1 Ma interval through GPlates and deciphered paleoclimate utilizing Scotese Global Climate Model [4].

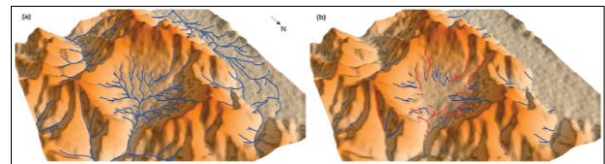


Fig.2. (a) Entire drainage pattern evolved from elevated rim of Xiuyan, (b) 1st order streams in red don't follow either radial or centripetal drainage pattern (Source: ALOS PALSAR elevation map over hill shade).

Results: The DI of 22 simple craters range from 0 to 0.80, while the DI of 49 complex craters range from 0.55 to 0.87 (Fig.3). With time, the denudation underwent by a crater increase, pointing to relatively low DI values for simple craters. Given the weak statistical correlation between age and DI, the paleoclimatic data of craters were correlated but the complexity of the crater denudation increases as craters experience multiple climates since formation.

Discussion: 1. *General Observations.* Simple craters formed on sedimentary and crystalline targets have an average DI of 0.26 and 0.47, while for complex craters the values are 0.73 and 0.79, respectively. The DI tend to be higher with greater duration of crater exposure to denudation agents since simple craters formed in Paleozoic have an average DI of 0.73, in Mesozoic have 0.71 and in Cenozoic have 0.31 whereas the DI is 0.71, 0.78 and 0.74, respectively for complex craters.

2. *Specific Observations.* (a) The extent of crater denudation increases in the order: warm temperate < subtropical arid < polar < cool temperate < equatorial rainy climate. (b) A relatively longer presence of craters in LDC (Low Denudational Climates) can equate to shorter durations in HDC (High Denudational Climates), pointing to higher denudation in HDC, irrespective of target rock types.

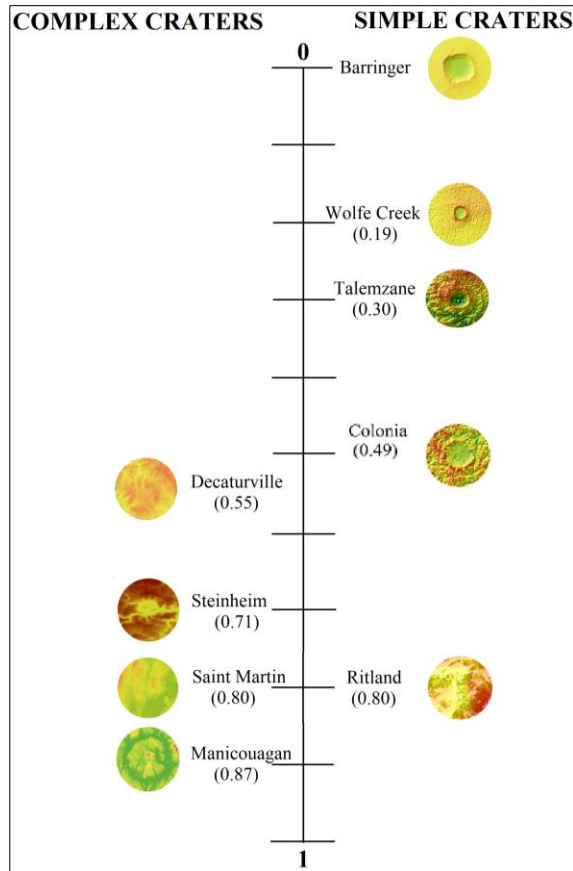


Fig.3. DI Scale of select terrestrial impact craters

3. Deviations from General and Specific Observations.

(a) The DI of younger craters ($DI_{\text{Hickman}}=0.67$) (0.02–0.10 Ma), at times can be higher than older craters ($DI_{\text{Tabun-Khara-Obo}}=0.64$) (150 ± 20 Ma). (b) The DI of craters formed on crystalline targets (such as $DI_{\text{Decaturville}}=0.55$) can be higher than ones formed at sedimentary targets ($DI_{\text{El'gygytgyn}}=0.87$). This observation deviates from the general trend of higher denudational vulnerability of sedimentary rocks than crystalline. Yet, the observation can be attributed to the brittle nature of crystalline rocks aiding more advanced fracture formation and thereby, more extensive and sophisticated drainage network development.

The deviations, further emphasize the dynamic nature of impact cratering on Earth, involving complex interactions between the projectile, target, resultant shock energies and ensuing post-impact denudational agents acting together with climate and time, to modify the impact structures as we see today.

References: [1] Gottwald, M. et al. (2020). Terrestrial Impact Structures. The TanDEM-X Atlas, Part 1 and 2. Verlag Dr. Friedrich Pfeil, Munich,

Germany. [2] Kenkmann, T., (2021). Meteorit. Planet. Sci. 56 (5), 1024–1070. [3] Schmieder, M. and Kring, D.A., (2020). Astrobiology, 20(1), 91–141 [4] Scotese, C.R. (2016). Global Climate Change Animation (540Ma to Modern), <https://youtu.be/DGf5pZMkjA0>.